Attenuation of Energy-based Demand Parameters

ALI SARI (asari@itu.edu.tr)

Istanbul Technical University - Ayazaga Campus: Istanbul Teknik Universitesi https://orcid.org/0000-0002-6888-1276

Lance MANUEL

UT Austin: The University of Texas at Austin

Research Article

Keywords: Input energy, Absorbed energy, Attenuation, Northwestern Turkey, Random effects

Posted Date: June 16th, 2021

DOI: https://doi.org/10.21203/rs.3.rs-615355/v1

ATTENUATION OF ENERGY-BASED DEMAND PARAMETERS

Ali SARI[a] **and Lance MANUEL**[b]
[a] Department of Civil Engineering,
Istanbul Technical University, Istanbul, 34610, TURKEY

[b]Department of Civil Engineering,
University of Texas at Austin, Austin, TX 78712, USA
*

ABSTRACT

The intensity of ground shaking and the demand on structures during earthquakes have been generally characterized using parameters such as peak ground acceleration as well as strength-based parameters such as response spectrum ordinates (e.g., spectral acceleration) that represent the maximum amplitude of shaking for structures with specified natural period and damping values. It has long been recognized that to assess the demands on structures during earthquakes, one might employ an energy-based approach (as an alternative to the more common strength-based one), especially when there is an interest in assessing damage potential of ground motions. An energy spectrum, obtained with the same level of effort required to construct a conventional response spectrum, is a convenient single-parameter description of both amplitude and duration of ground motion and can serve as a useful means by which to describe the performance of structures with different natural periods and damping ratios.

In this study, attenuation models for Northwestern Turkey are developed for two parameters (defined herein) that are related to input energy and absorbed energy. The empirical models developed take advantage of the recent increase in the database on strong motion data for Northwestern Turkey. A total of 195 recordings from 17 recent seismic events are included in this database. The ground-motion prediction equations developed are for the geometric mean of the two horizontal components of the 5-percent damped energy parameters (elastic and inelastic input energy-equivalent acceleration, A_i, and absorbed energy-equivalent velocity, A_a) at various periods. Predictions of the energy-based parameters from the proposed attenuation model are compared with (strength-based) spectral acceleration levels predicted by Özbey et al [Soil Dyn. & Earthq. Eng., 24 (2004), pp. 115-125]. It is found that the energy demand parameters were generally greater with elastic A_i demands highest. In addition, the predicted energy-based parameter levels are compared with available Western U.S. attenuation model predictions for the same energy-based parameters. Western U.S. models predict similar energy demands to those with the proposed model.

Finally, amplification factors for the energy-based parameters are proposed as a function of site class; these factors can be thought of as analogous to amplification factors for spectral acceleration as given in the NEHRP Seismic Provisions. The patterns related to the amplification are similar as with spectral

acceleration in NEHRP (2001). A comparison of soil amplification effects for strength- and energy-based parameters is also discussed.

KEYWORDS

Input energy; Absorbed energy; Attenuation; Northwestern Turkey; Random effects.

1. INTRODUCTION

Recent earthquakes have severely damaged relatively new buildings designed based on some strength or displacement-based methods (Shiwua and Rutman 2016). The severity of earthquake ground shaking is commonly characterized using intensity measures such as peak ground acceleration and spectral acceleration, which are force-based or strength-based parameters. It is aimed that the capacity of the structural elements is higher than the internal forces of the elements exposed to external loads in strength-based design methods (Merter, Bozda, and Düzgün 2012). Modern seismic provisions adopt such strength-based design procedures, where seismic demand is represented in the form of an elastic response spectrum. This design procedure indirectly tries to account the inelastic behavior during severe seismic excitation and through the force reduction factor based on ductility. One of the disadvantages of strength-based design is that the earthquake loading effect depends on the elastic and plastic properties of the structure and therefore manages the structural resistance (Shiwua and Rutman 2016). Design procedures, then, implicitly account for the ductility capacity that a structure might possess by the use of reduction factors, but they do not include in a direct way consideration of the cyclic nature of the response that the structure undergoes and the resulting cumulative damage. Earthquake resistant structures are designed using strength-based methods as well

as displacement-based and energy-based methods (Merter, Bozda, and Düzgün 2012). In contrast with such strength-based parameters, energy-based parameters may be just as easily defined but they can usefully include the effects of both the amplitude as well as the number of cycles of the response oscillations experienced by a structure. Such energy-based parameters are, as such, expected to correlate equally well or better with structural damage than the conventional strength-based parameters (Sari, 2003). In energy-based seismic design methods, elastic and inelastic seismic energy dissipations within structures are expected to be higher than the earthquake input energy and this method include more ground motion characteristics (Ma 2019; Merter, Bozda, and Düzgün 2012) One of the biggest differences between the energy-based seismic design method and other methods is that an energy dissipation mechanism is required in the design (Ye et al. 2009).

Ma et. al (Ma, Gu, and Sun 2019) researched energy-based seismic design based on source to site distance and site classification. According to the site classifications of Chinese seismic code, earthquake ground motion records were selected and the equivalent velocity spectra of hysteretic energy demand generated by the energy-balance equation. Decanini and Mollaioli (Decanini and Mollaioli 2001) proposed inelastic energy spectra as a function of ductility, soil type, source-to-site distance and magnitude and the energy-based spectra of the hysteretic to input energy ratio were evaluated, for different soil types and target

ductility ratios. Ozsarac et al. (Ozsarac et al. 2017) derived ground motion data on the North Anatolian Fault by simulating moment magnitude, distance and soil conditions. The characteristics of elastic and inelastic input energies and the percentage of hysteretic energy were investigated. The authors believe that the simulated ground motions will encourage and facilitate energy-based design. Almansa et. al (López-Almansa, Yazgan, and Benavent-Climent 2013) proposed design energy input spectra in terms of equivalent velocity. In this study, Turkish strong ground motions were selected and these records were divided into groups according to soil type and magnitude. Empirical criteria for estimating the ratio between hysteretic energy in terms of velocity and input energy are represented. Compared with those from other studies, the proposed design spectra are noted to be larger in some cases and smaller in others. Dindar et. al (Dindar et al. 2013) proposed an energy demand spectrum, taking into account the structural properties and site conditions. In this study, in order to understand the effect of ground motion characteristics such as site conditions on seismic energy demand, the energy balance equation is examined.

Of interest here is a study of the attenuation of energy-based ground motion parameters where a random effects model is employed that takes into consideration the correlation of data recorded by a single event (Abrahamson and Youngs, 1992). As a result of the recent increase in the database on strong

motion data for Northwestern Turkey and because there exists currently only a very limited number of ground-motion prediction equations in the world for energy-based parameters, we seek to develop new region-specific energy-based ground-motion prediction equations for Northwestern Turkey. In addition, there are similarities in characteristics of San Andreas Fault, California and North Anatolian Fault (NAF), which is the main fault system that caused several severe earthquakes in Northwestern Turkey (Ambraseys, 1970, Dewey, 1976 and Çelebi et al, 1999). A database consisting of 195 recordings from 17 recent seismic events is employed for this purpose. This database is the same as that employed by Özbey et al (2004).

The ground-motion prediction equations developed are for the geometric mean of the two horizontal components of 5-percent damped energy parameters that will be defined in the following. For elastic energy demand as well as for different inelastic energy demand levels (associated with a range of ductility values), results are reported. For a subset of the cases studied that are thought to be of most interest, period-dependent attenuation model coefficients based upon the random effects model used are presented in tabular form to facilitate their use.

The effect of magnitude, soil class, and distance on the predicted energy spectra is studied. The effect of ductility level is also studied. Model predictions for the energy parameters are studied in detail and compared with observed data

for the different soil classes. The proposed ground-motion prediction equations are also compared with the few available Western U.S. attenuation models for energy-based parameters. There is virtually no previous work published on amplification of energy-based parameters due to site conditions except a brief study carried out by Chou and Uang (2000). A similar brief examination of the attenuation of short- and long-period motions based on energy considerations for different site/soil classes permits us to present soil amplification factors for energy-based ground motion parameters here.

2. MODEL PARAMETERS AND STRONG MOTION DATABASE

The model parameters included to establish the empirical attenuation models in this study are that same as those employed by Özbey et al. (2004). These parameters include earthquake moment magnitude, M_w; the Joyner-Boore source-to-site distance (Boore and Joyner, 1982), R (a measure of the closest horizontal distance to the vertical projection of the rupture plane); and local site conditions (as specified by different site classes described in the following). It should be noted that style of faulting is not explicitly included as a model parameter. The empirical ground-motion prediction equations developed are for normal and strike-slip earthquakes and should not be used for reverse and reverse-oblique events since the fault mechanisms for earthquakes on the North Anatolian

Fault System (including most of the Kocaeli aftershocks) are predominantly strike-slip in character with normal faulting observed in some cases (Orgulu and Aktar, 2001). Records from aftershocks were also used by Abrahamson and Silva (1997) in their attenuation relationship, which is widely used by the engineering and the seismological society.

A database made up of 195 ground motion records from 17 earthquakes (main shocks and aftershocks with magnitude greater than 5.0) is employed here. The restrictions discussed below reduced the number of records used in this study to 195 from 1188 records. The strong motion dataset is restricted to earthquakes with Mw≥ 5 to get more reliable predictions of ground motions. Using a lower magnitude limit, like Mw≥ 4, would increase the number of records in the analyzed dataset. However an additional error would be introduced to the attenuation relationship, as for the small earthquakes spectral values could be affected by the band-pass filter used for noise removal. These records comprise a subset of a larger database of events of various magnitudes that were obtained from stations operated by Boğaziçi University's Kandilli Observatory and Earthquake Research Institute (KOERI), by Istanbul Technical University (ITU), and by the General Directorate of Disaster Affairs' Earthquake Research Department (ERD). Baseline correction is applied by first removing the mean from the acceleration record and then fitting a second order polynomial to the

velocity record. Derivative of the fitted polynomial is subtracted from the acceleration record. Acausal filters are used to eliminate the noise from the records. Corner frequencies are selected based on visual examination of the records. No screening process is employed in the study.

Table 1 includes a summary of the records included in the selected strong motion database (which is the same as that used by Sari (2003) and Özbey et al. (2004). Only earthquakes occurred in the western part of the North Anatolian Fault is included in the dataset as the aim was to develop a regional attenuation relationship for Northwestern Turkey. Also for the same reason, only the strong motion stations located in Northwestern Turkey are included in the dataset.

The distribution the database is based on site classes A, B, C, and D as defined in Table 2 is also shown. Site classifications proposed by Rathje et al (2003) are used. The site classifications are based on the V_{30} measurements and SASW testing has been performed to measure the V_{30} values.

The magnitude predictions from the Seismology department of Kandilli Observatory of Boğaziçi University are utilized in the study.

Table 1: Database of strong motion records used in the regression analyses.

Event No	*Event Name*	*Event Date*	*Origin Time*	*Lat. (deg.)*	*Long. (deg.)*	*M*	*H (km)*	*No. of Recordings*			
								A	*B*	*C*	*D*
1	"Kocaeli"	17.08.1999	12:01:38 AM	40.76	29.97	7.4	19.6	3	5	7	7
2	"Düzce-Bolu"	12.11.1999	4:57:21 PM	40.74	31.21	7.2	25.0	1	3	5	18
3	"Kocaeli"	13.09.1999	11:55:29 AM	40.77	30.10	5.8	19.6	0	2	5	18
4	"Hendek-Akyazi"	23.08.2000	1:41:28 PM	40.68	30.71	5.8	15.3	0	1	3	8
5	"Sapanca-Adapazari"	11.11.1999	2:41:26 PM	40.74	30.27	5.7	22.0	0	1	4	11

6	"Kocaeli"	17.08.1999	3:14:01 AM	40.64	30.65	5.5	15.3	0	0	0	3
7	"Düzce-Bolu"	12.11.1999	5:18:00 PM	40.74	31.05	5.4	10.0	0	1	1	12
8	"Kocaeli"	31.08.1999	8:10:51 AM	40.75	29.92	5.2	17.7	0	1	3	13
9	"Düzce-Bolu"	12.11.1999	5:17:00 PM	40.75	31.10	5.2	10.0	0	2	1	11
10	"Marmara Sea	20.09.1999	9:28:00 PM	40.69	27.58	5.0	16.4	0	1	4	10
11	"Northeast of Bolu'	14.02.2000	6:56:36 AM	40.90	31.75	5.0	15.7	0	0	0	5
12	"Cinarcik-Yalova"	19.08.1999	3:17:45 PM	40.59	29.08	5.0	11.5	0	0	1	5
13	"Kaynasli-Bolu"	12.11.1999	6:14:00 PM	40.75	31.36	5.0	10.0	0	0	0	1
14	"Hendek-Adapazari"	07.11.1999	4:54:42 PM	40.71	30.70	5.0	10.0	0	0	0	4
15	"Kocaeli"	19.08.1999	3:17:45 PM	40.36	29.56	5.0	9.8	0	1	1	2
16	"Düzce-Bolu"	19.11.1999	7:59:08 PM	40.78	30.97	5.0	9.2	0	2	0	3
17	"Hendek-Adapazari"	22.08.1999	2:30:59 PM	40.74	30.68	5.0	5.4	0	0	0	5
							Total Number of Records :	4	20	35	136

Table 2: Definition of site classes used in the attenuation model development.

Site Class	Shear wave velocity
A	> 1500 m/s
B	760 m/s to 1500 m/s
C	360 m/s to 760 m/s
D	180 m/s to 360 m/s

The distribution of the strong motion data as a function of moment magnitude and distance is shown graphically according to site class in Fig. 1. Note that the site classes A and B have been included together in this figure.

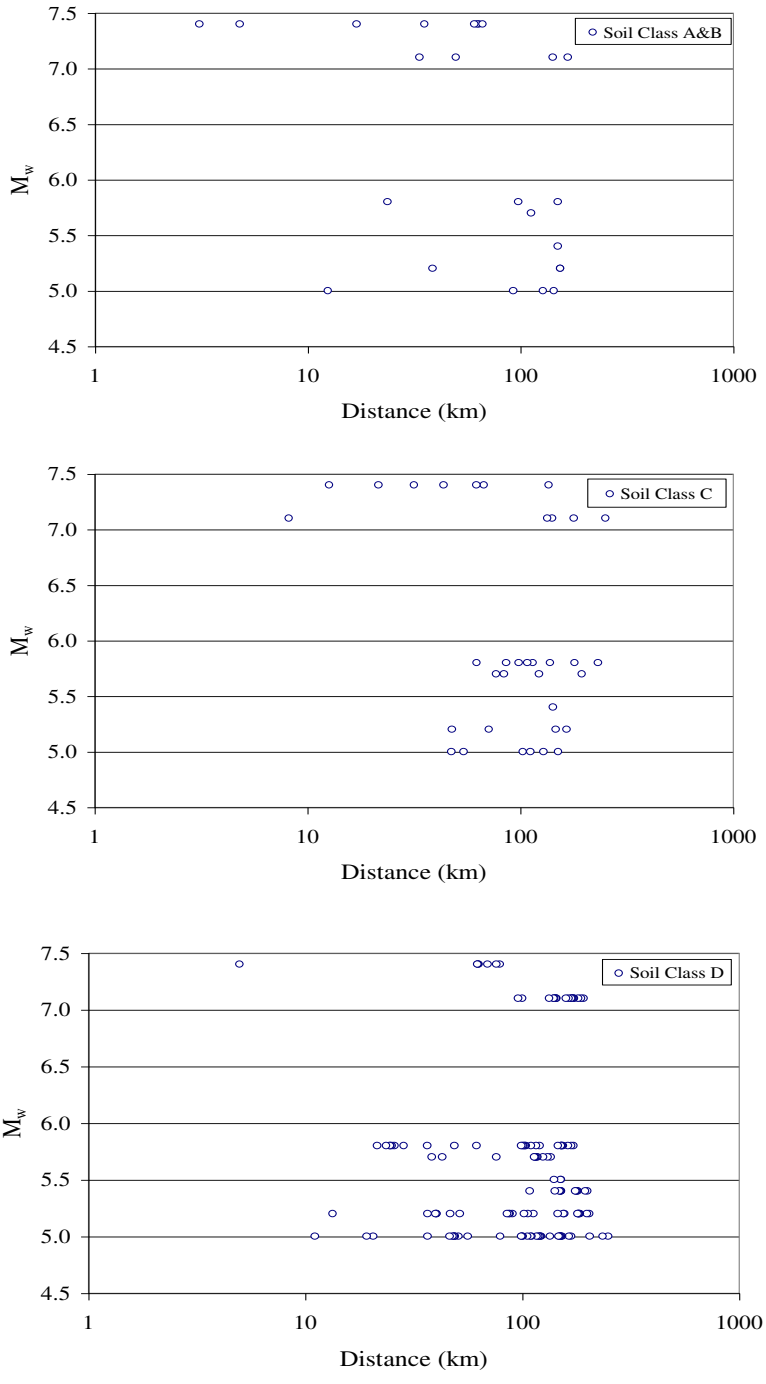

Figure 1: Data Distribution for Soil Classes (A&B), C and D.

3. BACKGROUND ON ENERGY-BASED GROUND MOTION PARAMETERS

Ground motions may be described quantitatively in different terms when one is interested in understanding their effect on structures with different natural period and damping values. Conventionally, strength-based parameters (such as spectral acceleration (S_a) or velocity (S_v) or even peak ground acceleration) have been used for this purpose. Regression-based models describing the attenuation of these parameters as a function of magnitude and distance (for specified site conditions and sometimes by faulting type) have been developed for various regions of the world. Not as extensively studied are energy-based ground motion parameters and models describing their attenuation.

It is only in recent studies that energy-based measures of ground shaking have gained interest. Since there are several different such energy descriptors that have been used, it is important to define the energy-based parameters that are employed here. In order to do so, it is useful to start with the equation of motion of a single-degree-of-freedom structural (SDOF) system. This may be written as:

$$m\ddot{u}_t + c\dot{u} + f_s = 0 \tag{1}$$

where m, c, and f_s are the mass, viscous damping coefficient, and restoring force, respectively, of the SDOF system. Also, u_t is the absolute (total) displacement of

the mass, while $u = u_t - u_g$ is the relative displacement of the mass with respect to ground, and u_g is the ground displacement.

Transformation of the equation of motion into an energy balance equation can be easily accomplished by integrating Eq. (1) with respect to u from the beginning of the input ground motion (see, for example, Uang and Bertero, 1988). This leads to:

$$\frac{m\dot{u}_t^2}{2} + \int_0^t c\dot{u}\,du + \int_0^t f_s\,du = \int_0^t m\ddot{u}_t\,du_g \tag{2}$$

Since the inertia force, $m\ddot{u}_t$, equals the sum of the damping and restoring forces, it is also equal to the total force applied at the base of the structure. Therefore, the right-hand side of Eq. (2) is, by definition, the energy input to the system at any time, t. Hereinafter, following Uang and Bertero (1988), we will define Input Energy, E_i, as the *maximum* value of the energy input into the system during ground shaking. It can also be thought of as the maximum value of the work done by the total base shear on foundation/ground displacement during the ground motion. Thus, we have:

$$E_i = \max\left\{\int_0^t m\ddot{u}_t\,du_g\right\} \tag{3}$$

The first term on the left hand side of Eq. (2) is the *kinetic energy*, $E_k(t)$, while the second term is the *damping energy*, $E_d(t)$, and the last term is made up

of the sum of recoverable *elastic strain energy*, $E_s(t)$, and irrecoverable *hysteretic energy*, $E_h(t)$. Thus, the input energy, E_i, can also be described as follows:

$$E_i = \max\left\{\frac{m\dot{u}_t^2}{2} + \int_0^t c\dot{u}\,du + \int_0^t f_s\,du\right\} = \max\left\{E_k(t) + E_d(t) + \left[E_s(t) + E_h(t)\right]\right\} \quad (4)$$

Similarly, to facilitate reporting of various results in this study and comparisons with other studies, it is useful to define (as is done by Uang and Bertero (1988)), Absorbed Energy, E_a, as the maximum value of the sum of the recoverable strain energy and the irrecoverable hysteretic energy as follows:

$$E_a = \max\left\{\int_0^t f_s\,du\right\} = \max\left\{E_s(t) + E_h(t)\right\} \quad (5)$$

It is convenient to define a velocity parameter (V_i) based on input energy which we will term, "input energy-equivalent velocity":

$$V_i = \sqrt{\frac{2E_i}{m}} \quad (6)$$

Similarly, we define another velocity parameter (V_a) based on absorbed energy which we will term, "absorbed energy-equivalent velocity":

$$V_a = \sqrt{\frac{2E_a}{m}} = \sqrt{\frac{2(E_s + E_h)}{m}} \quad (7)$$

Also, to facilitate comparison with studies that involve the more conventional design parameter, spectral acceleration, S_a, we define an "input energy-equivalent acceleration," A_i, in terms of V_i and an "absorbed energy-equivalent acceleration," A_a, in terms of V_a, as follows:

$$A_i = \omega V_i ; \quad A_a = \omega V_a \tag{8}$$

Of these various parameters, input energy-equivalent velocity, V_i, was used as a ground motion parameter in attenuation studies for the Western U.S. by Lawson (1996) and Chapman (1999); the latter study also included the use of elastic input energy-based parameters in probabilistic seismic hazard analyses. Also, inelastic absorbed energy-equivalent velocity was employed as an energy demand parameter in a recent study on attenuation by Chou and Uang (2000).

It is important to note that for linear elastic systems, the absorbed energy-equivalent velocity, V_a, is the same as spectral velocity, S_v, and the absorbed energy-equivalent acceleration, A_a, is the same as spectral acceleration, S_a. Thus, in a sense, elastic absorbed energy-equivalent velocity and acceleration represent parameters that may be defined either from strength or energy considerations.

4. REGRESSION MODEL

A nonlinear mixed effects model is employed in the development of the ground-motion prediction equations in this study. Such a model can account for both inter-event and intra-event variability. Most of the attenuation models do not

distinguish between these two types of variability. The mixed effects model used here has been discussed extensively by Özbey et al. (2004) and by Sari (2003). Such a model describes the relationship between a response variable, the ground motion parameter, and some covariates in the data that are grouped according to one or more classification (for example, magnitude).

The error associated with residuals between predicted and observed values of the selected ground motion parameter is comprised of an inter-event term (that represents between-group variability resulting from differences in the data recorded from different earthquakes) and an intra-event term (that represents within-group variability resulting from differences in the data recorded among the different stations for the same earthquake).

The selected functional form for the ground-motion prediction equations that are developed for elastic and inelastic energy-based ground motion parameters using the mixed effects model is as follows:

$$\log(Y_{ij}) = a + b(M_i - 6) + c(M_i - 6)^2 + d\log\sqrt{R_{ij}^2 + h^2} + eG_1 + fG_2 \qquad (9)$$

where Y_{ij} is the geometric mean of the two horizontal components of the energy-based parameter (e.g., A_i or A_a in units of cm/s^2) from the j^{th} recording of the i^{th} event, M_i is the moment magnitude of the i^{th} event, and R_{ij} is the closest horizontal distance to the vertical projection of the rupture from the i^{th} event to the location of the j^{th} recording. However, it is known that the quadratic function of

magnitude in place in the equation to incorporate magnitude saturation and the data are primarily at the both ends of the magnitude range, the quadratic term is preferred to keep in the equation instead of leaving out the term because the equation that is used in this study is widely known and accepted by the researchers.

The coefficients G_1 and G_2 take on values as follows: G_1=0 and G_2=0 for site classes A and B; G_1=1 and G_2=0 for site class C; and G_1=0, G_2=1 for site class D. The coefficients to be estimated are, hence, a, b, c, d, e, f, and h. Note that the regression coefficients are not smoothed.

5. REGRESSION RESULTS

To facilitate comparisons with spectral acceleration, regression results for the energy parameters are presented and discussed in terms of absorbed energy-equivalent acceleration (A_a) and input energy-equivalent acceleration (A_i) defined based on Eq. (8). Our interest is in predictions of both elastic and inelastic measures of energy. However, it has been reported that absorbed energy is a better measure of damage to structures than input energy (see Chou and Uang, 2000); accordingly, when we are interested in inelastic demand, we will focus on absorbed energy-equivalent acceleration, A_a. For elastic energy demand, on the other hand, we will study input energy-equivalent acceleration, A_i. It is not necessary to consider elastic A_a because it is exactly the same as spectral

acceleration, S_a (ground-motion prediction equations for which have already been developed by Özbey et al (2004)). To summarize then, inelastic A_a and elastic A_i attenuation is discussed in the following.

Note that the evaluation of absorbed energy-equivalent acceleration (A_a) and input energy-equivalent acceleration (A_i) is limited to SDOF systems with 5% damping. Also, whenever inelastic structural response is of interest in the following, bilinear force-deformation characteristics with a 0% strain hardening ratio (or, equivalently, elastic perfectly-plastic behavior) are considered. The degree of strain hardening has been found to have insignificant influence on absorbed energy demands as has been reported by Chou and Uang (2000) and Seneviratna and Krawinkler (1997). This was also discussed by Sari and Manuel (2002). Hence, no other strain hardening ratios are considered.

5.2. Absorbed Energy

Based on the mixed effects model, Table 3 presents the attenuation coefficients, a, b, c, d, e, f, and h, and the logarithmic standard error for 5%-damped inelastic absorbed energy-equivalent acceleration (A_a) for periods up to 4 seconds and for a ductility factor of 4. (A ductility factor of 4 implies that the SDOF system experiences a maximum displacement that is 4 times the yield displacement.)

Table 3: Empirical attenuation coefficients and logarithmic standard deviation for the 5%-damped absorbed energy-equivalent acceleration, A_a (in cm/s^2) for ductility = 4.

Period (s)	***a***	***b***	***c***	***d***	***h***	***e***	***f***	$\sigma_{\log(Y)}$
0.10	3.742	0.510	-0.085	-1.0526	13.01	0.133	0.284	0.246
0.15	3.643	0.523	-0.083	-0.9856	12.66	0.112	0.278	0.236
0.20	3.517	0.556	-0.106	-0.9176	11.92	0.078	0.304	0.228
0.25	3.320	0.582	-0.111	-0.8343	8.80	0.071	0.325	0.232
0.30	3.219	0.602	-0.116	-0.8039	8.71	0.077	0.349	0.235
0.35	3.132	0.616	-0.119	-0.7789	8.15	0.076	0.360	0.239
0.40	3.071	0.628	-0.126	-0.7681	8.26	0.078	0.377	0.245
0.45	2.996	0.639	-0.127	-0.7457	7.74	0.073	0.383	0.251
0.50	2.943	0.648	-0.129	-0.7372	7.47	0.074	0.393	0.255
0.55	2.887	0.655	-0.128	-0.7257	7.51	0.074	0.400	0.258
0.60	2.839	0.660	-0.128	-0.7178	7.57	0.076	0.404	0.258
0.65	2.810	0.665	-0.130	-0.7180	7.75	0.077	0.408	0.261
0.70	2.782	0.669	-0.131	-0.7187	7.67	0.079	0.411	0.262
0.75	2.761	0.675	-0.132	-0.7194	7.80	0.081	0.414	0.263
0.80	2.740	0.677	-0.134	-0.7212	7.85	0.083	0.415	0.264
0.85	2.715	0.683	-0.136	-0.7194	8.00	0.085	0.420	0.266
0.90	2.693	0.687	-0.137	-0.7198	8.05	0.088	0.425	0.267
0.95	2.672	0.690	-0.139	-0.7202	8.12	0.089	0.427	0.268
1.00	2.660	0.693	-0.142	-0.7231	8.30	0.090	0.429	0.268
1.10	2.630	0.696	-0.145	-0.7266	8.41	0.090	0.431	0.267
1.20	2.605	0.700	-0.148	-0.7309	8.46	0.091	0.433	0.267
1.30	2.588	0.703	-0.151	-0.7373	8.61	0.091	0.433	0.267
1.40	2.566	0.706	-0.153	-0.7403	8.70	0.091	0.433	0.268
1.50	2.548	0.708	-0.154	-0.7452	8.88	0.092	0.434	0.268
1.75	2.512	0.713	-0.159	-0.7574	9.11	0.092	0.436	0.268
2.00	2.469	0.715	-0.161	-0.7629	9.25	0.091	0.436	0.268
2.25	2.431	0.717	-0.161	-0.7670	9.33	0.085	0.432	0.267
2.75	2.356	0.720	-0.158	-0.7697	9.57	0.077	0.425	0.266
3.00	2.326	0.722	-0.157	-0.7725	9.53	0.075	0.423	0.266
3.50	2.275	0.726	-0.156	-0.7792	9.31	0.075	0.421	0.265
4.00	2.232	0.728	-0.154	-0.7846	9.44	0.072	0.417	0.265

Figure 2 shows absorbed energy-equivalent acceleration spectra based on model predictions for four different ductility levels for soil classes A and B when

M_w = 7.5 and R = 10 km. Insignificant differences in absorbed energy-equivalent acceleration (A_a) are observed for ductility levels in the inelastic range from 2 to 8, except at very short periods. Recognizing this lack of sensitivity of absorbed energy demands to ductility levels, in the following while discussing inelastic A_a attenuation, only a ductility factor of 4 is studied.

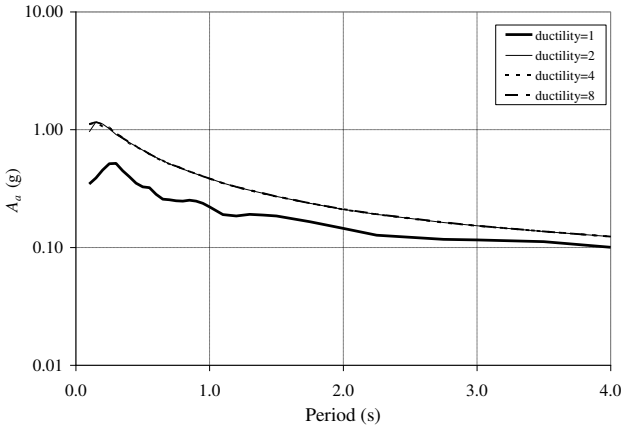

Figure 2: Effect of ductility on predicted absorbed energy-equivalent acceleration spectra for M_w=7.5, R =10 km, and for soil classes A and B.

The effect of magnitude on predicted inelastic absorbed energy-equivalent acceleration spectra is studied in Fig. 3 for soil classes A and B for R = 20 km, and for a ductility factor of 4. A systematic decrease in amplitude of the spectra with decreasing magnitude is observed at all frequencies as expected. Figure 4 shows the effect of soil class on inelastic absorbed energy-equivalent acceleration spectra based on the proposed attenuation model predictions for M_w = 7.5 and R = 10 km and for a ductility factor of 4. For all soil classes, it may be seen that the

inelastic (ductility = 4) A_a has its peak value at a period lower than 0.25 seconds, which is somewhat shorter than the period of 0.3 seconds at which the elastic A_a (or spectral acceleration) has its own peak value as can be seen in Özbey et al (2004). The effect of distance on predicted inelastic absorbed energy-equivalent acceleration spectra is studied in Fig. 5 for soil classes A and B for M_w = 7.5 and for a ductility factor of 4. An expected trend of reduced ground motion attenuation with distance is seen at longer periods.

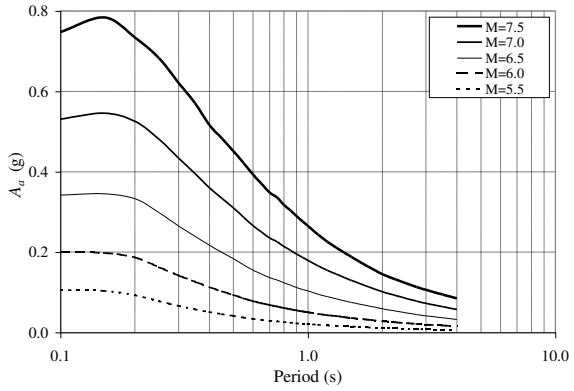

Figure 3: Effect of magnitude on predicted inelastic absorbed energy-equivalent acceleration spectra for soil classes A and B, R = 20 km, and ductility factor = 4.

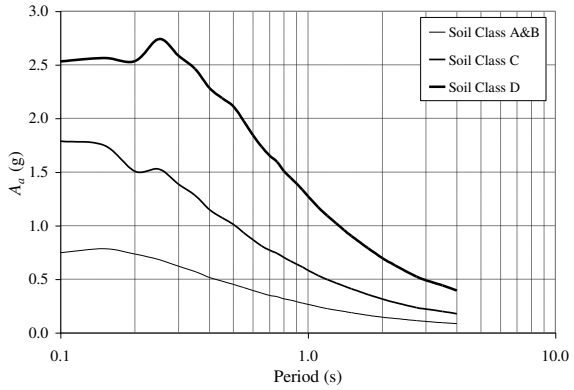

Figure 4: Effect of soil class on predicted inelastic absorbed energy-equivalent acceleration spectra for M_w=7.5, R =10 km, and ductility factor = 4.

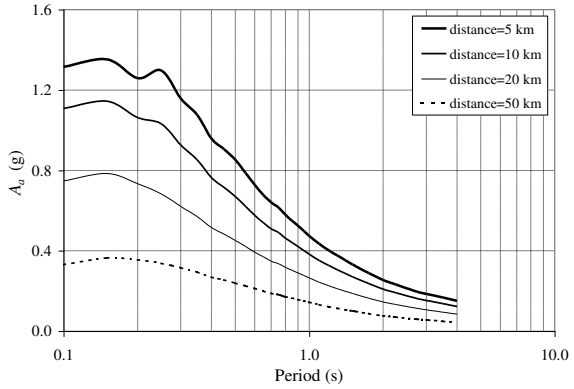

Figure 5: Effect of distance on predicted inelastic absorbed energy-equivalent acceleration spectra for soil classes A and B and for M_w=7.5 and ductility factor = 4.

In Fig. 6, model predictions of inelastic (ductility = 4) 1.0-second absorbed energy-equivalent acceleration (A_a) for mean and plus/minus one standard deviation levels are compared with data from the Kocaeli earthquake. To highlight the differences in the predicted motions for each soil class, the

comparisons for soil classes (A&B), C, and D are shown separately. Reasonable fits of the model to the Kocaeli data are seen in Fig. 6.

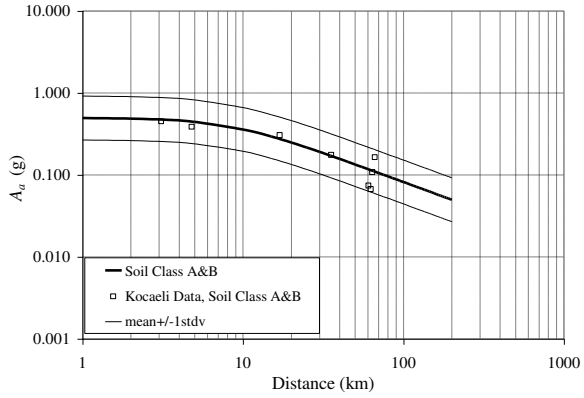

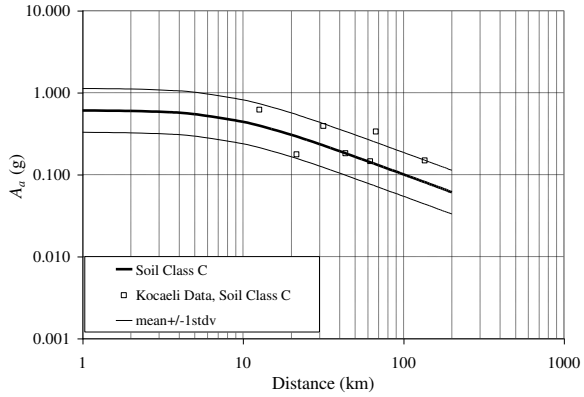

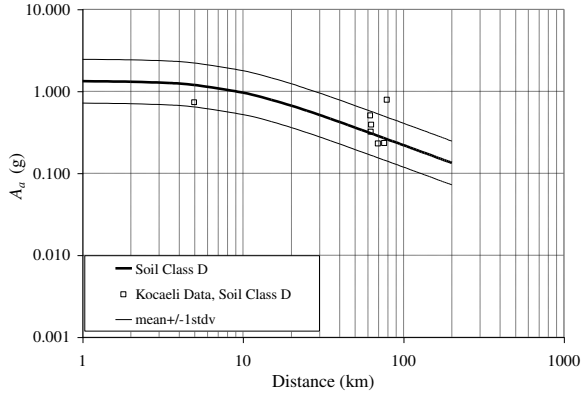

Figure 6: Comparison of model predictions of 1.0-second inelastic (ductility = 4) A_a at mean and mean ± 1 std. dev. levels with observed data from the Kocaeli earthquake (M_w=7.4) for soil classes (A&B), C, and D.

5.2. Input Energy

Based on the mixed effects model, Table 4 presents the attenuation coefficients, *a*, *b*, *c*, *d*, *e*, *f*, and *h*, and the logarithmic standard error for 5%-damped elastic input energy-equivalent acceleration (A_i) for periods up to 4 seconds.

Table 4: Empirical attenuation coefficients and logarithmic standard deviation for the 5%-damped elastic input energy-equivalent acceleration, A_i (in cm/s^2).

Period (s)	***a***	***b***	***c***	***d***	***h***	***e***	***f***	$\sigma_{log(Y)}$
0.10	3.877	0.614	-0.084	-1.0480	9.95	0.115	0.267	0.250
0.15	4.042	0.588	-0.096	-1.1460	16.61	0.171	0.271	0.243
0.20	3.745	0.582	-0.085	-1.0063	13.87	0.094	0.273	0.227
0.25	3.497	0.595	-0.090	-0.8887	10.21	0.039	0.278	0.231
0.30	3.376	0.602	-0.102	-0.8421	7.99	0.035	0.288	0.237
0.35	3.278	0.623	-0.124	-0.8092	6.88	0.033	0.323	0.240
0.40	3.127	0.632	-0.115	-0.7716	5.99	0.055	0.367	0.260
0.45	3.028	0.649	-0.133	-0.7335	5.43	0.062	0.388	0.268
0.50	2.943	0.687	-0.168	-0.6906	4.59	0.036	0.390	0.286
0.55	2.844	0.718	-0.186	-0.6534	3.56	0.023	0.397	0.301
0.60	2.706	0.730	-0.184	-0.6037	2.80	0.022	0.396	0.305
0.65	2.609	0.737	-0.179	-0.5784	2.30	0.024	0.405	0.300
0.70	2.563	0.744	-0.180	-0.5711	2.09	0.020	0.405	0.299
0.75	2.554	0.769	-0.187	-0.5909	2.62	0.029	0.411	0.305
0.80	2.548	0.775	-0.185	-0.6072	3.08	0.045	0.407	0.308
0.85	2.565	0.800	-0.184	-0.6374	4.71	0.066	0.416	0.318
0.90	2.586	0.813	-0.190	-0.6627	6.33	0.071	0.425	0.326
0.95	2.583	0.828	-0.203	-0.6696	6.96	0.071	0.431	0.334

1.00	2.592	0.842	-0.221	-0.6807	6.69	0.069	0.433	0.334
1.10	2.585	0.857	-0.247	-0.6914	6.23	0.071	0.435	0.335
1.20	2.590	0.873	-0.273	-0.7117	6.13	0.086	0.444	0.336
1.30	2.626	0.893	-0.285	-0.7452	6.58	0.070	0.416	0.332
1.40	2.665	0.917	-0.294	-0.7821	7.94	0.050	0.404	0.339
1.50	2.670	0.933	-0.297	-0.7992	9.23	0.032	0.376	0.350
1.75	2.746	0.952	-0.320	-0.8832	10.04	0.031	0.343	0.351
2.00	2.710	0.956	-0.322	-0.9258	9.43	0.050	0.350	0.337
2.25	2.782	0.962	-0.320	-1.0119	12.42	0.049	0.355	0.329
2.75	2.663	0.956	-0.268	-1.0467	12.89	0.032	0.331	0.314
3.00	2.623	0.968	-0.260	-1.0540	13.01	0.034	0.324	0.316
3.50	2.545	0.972	-0.256	-1.0674	10.36	0.023	0.311	0.318
4.00	2.438	0.986	-0.244	-1.0699	10.41	0.014	0.315	0.309

Even though we do not study inelastic input energy demand in any detail in the following (for reasons already stated), we briefly examine the effect of ductility level on input energy-equivalent acceleration (A_i) spectra first. Figure 7 shows these A_i spectra based on model predictions for four different ductility levels for soil classes A and B when M_w = 7.5 and R = 10 km. Again, as was the case when studying A_a, insignificant differences in input energy-equivalent acceleration (A_i) are observed for all ductility levels ranging from 1 (elastic) to 8.

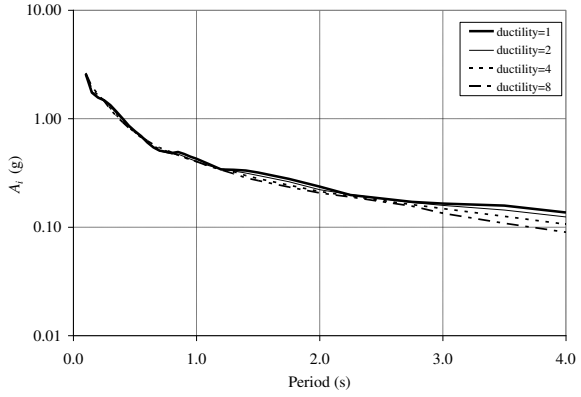

Figure 7: Effect of ductility on predicted input energy-equivalent acceleration spectra for M_w=7.5, R =10 km, and for soil classes A and B.

The effect of magnitude on predicted elastic input energy-equivalent acceleration spectra is studied in Fig. 8 for soil classes A and B for R = 20 km. A systematic decrease in amplitude of the spectra with decrease in magnitude is observed at all frequencies as expected. The shapes of the spectra are such that peak values of elastic A_i occur at the shortest periods unlike spectra for spectral acceleration which have peaks at intermediate periods generally. Figure 9 shows the effect of soil class on elastic input energy-equivalent acceleration spectra based on the proposed attenuation model predictions for M_w = 7.5 and R = 10 km. Again, it may be seen that the elastic A_i is largest at very short periods for all soil classes. The effect of distance on predicted elastic input energy-equivalent acceleration spectra is studied in Fig. 10 for soil classes A and B for M_w = 7.5. The expected trend of reduced ground motion attenuation with distance is seen at longer periods as was also observed for A_a spectra.

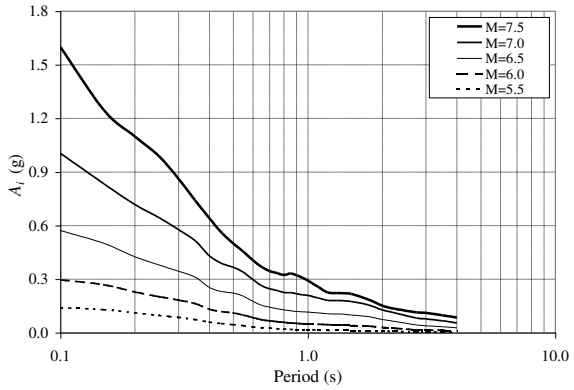

Figure 8: Effect of magnitude on predicted elastic input energy-equivalent acceleration spectra for soil classes A and B and for R = 20 km.

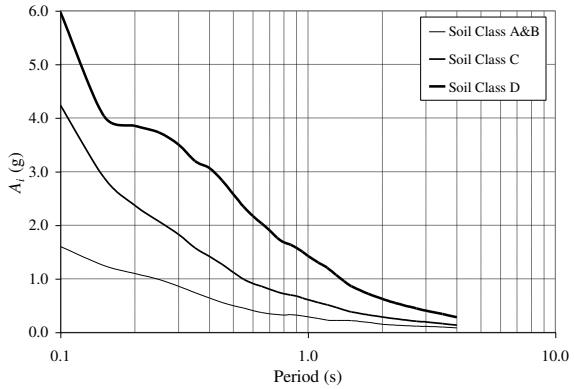

Figure 9: Effect of soil class on predicted elastic input energy-equivalent acceleration spectra for M_w=7.5 and R =10 km.

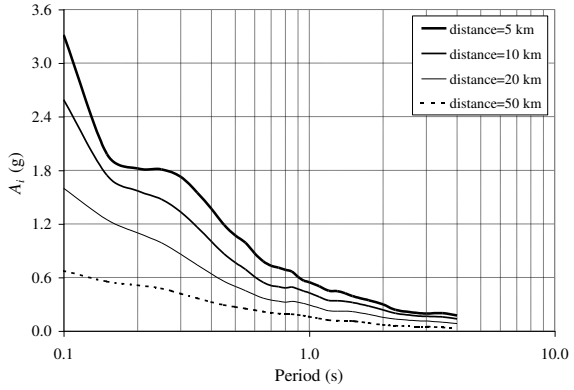

Figure 10: Effect of distance on predicted elastic input energy-equivalent acceleration spectra for soil classes A and B and for M_w=7.5.

In Fig. 11, model predictions of elastic 1.0-second input energy-equivalent acceleration (A_i), for mean and plus/minus one standard deviation levels are compared with data from the Kocaeli earthquake for soil classes (A&B), C, and D. Reasonable fits of the model to the Kocaeli data are seen in Fig. 11. The elastic A_i levels for the various soil classes are comparable with each other (highest levels are seen for soil class D) and somewhat higher than the levels of inelastic A_a (for a ductility of 4) that were seen in Fig. 6.

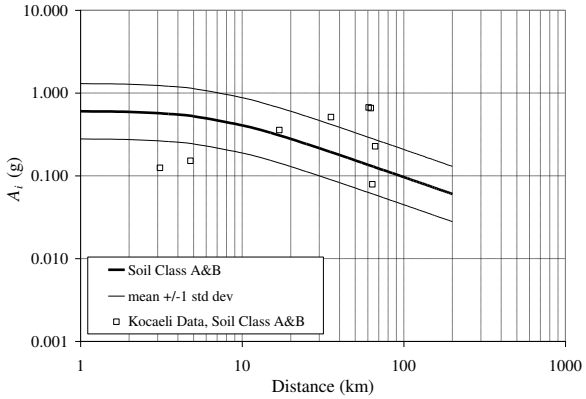

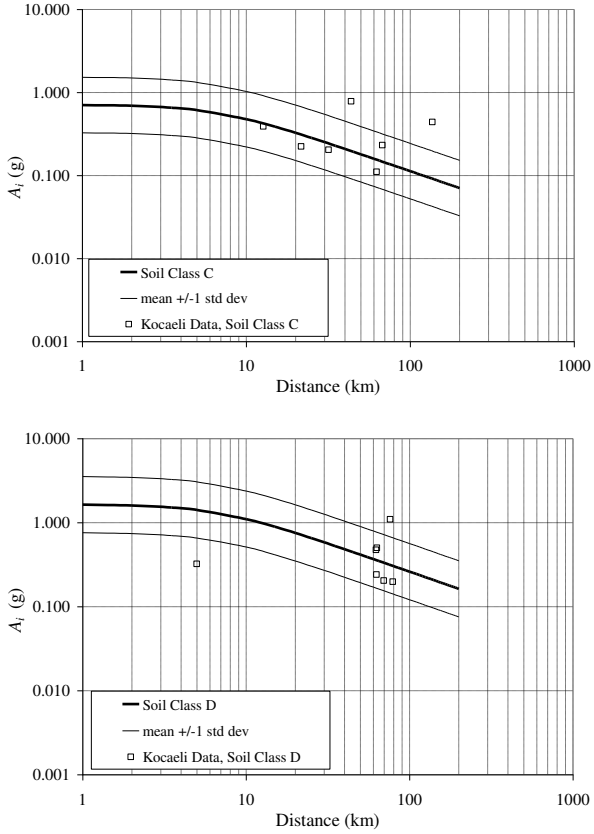

Figure 11: Comparison of model predictions of 1.0-second elastic A_i at mean and mean ± 1 std. dev. levels with observed data from the Kocaeli earthquake (M_w=7.4) for soil classes (A&B), C, and D.

6. DISCUSSIONS

We discuss three different issues next related to the attenuation of energy-based parameters studied. First, we compare the attenuation of the energy-based acceleration parameters, A_a and A_i, discussed in the preceding with the attenuation of spectral acceleration (from Özbey et al (2004)) based on the same ground motion database. Second, we discuss how predictions of attenuation of energy-

based parameters based on the empirical relationships developed here for Northwestern Turkey compare with ground-motion prediction equations developed using a Western U.S. strong motion database. Finally, we discuss how the ground-motion prediction equations developed may be employed to gain an understanding of the amplification of energy demands based on site conditions.

6.1. Comparison of the Predicted Attenuation of Strength- and Energy-Based Parameters

Predicted spectral acceleration levels for Northwestern Turkey, based on the study by Özbey et al (2004), and levels of absorbed energy-equivalent acceleration, A_a (for a ductility of 4) as well as elastic input energy-equivalent acceleration (A_i), based on the proposed attenuation model are compared in Figs. 12 and 13 for natural periods of 0.1 and 1.0 second, respectively. These comparisons are for an event with moment magnitude, M_w, equal to 7.4 and for soil classes A and B. The attenuation of motions with distance is shown in the figures.

It may be observed that the ratio of A_a (for a ductility of 4) to S_a is higher at short periods (see Fig. 12 for the 0.1 second period) compared to intermediate or long periods (see Fig. 13). When the response is elastic (ductility equal to 1), A_a is the same as S_a and the A_a/S_a ratio is unity; with increasing ductility this ratio increases. For a ductility factor of 4, the A_a/S_a ratio is about 3.3 at a distance of

10 km for a 0.1 second natural period, while the ratio is only about 1.5 at the same distance when the natural period is increased to 1 second. It is clear that predicted A_a levels should increase with ductility because hysteretic energy (E_h) contributes relatively a greater proportion to the total absorbed energy as ductility levels increase (whereas in the elastic case, E_h is equal to 0). Predicted A_i levels are higher than both A_a and S_a at the two periods, 0.1 and 1.0 seconds. However, the predicted levels for A_a and A_i are more similar to each other at the 1.0 second period than at the 0.1 second period.

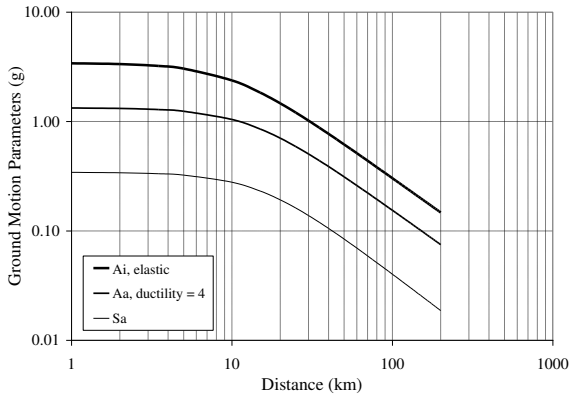

Figure 12: Comparison of 0.1-second elastic input energy-equivalent acceleration and inelastic (ductility = 4) absorbed energy-equivalent acceleration predictions from the proposed attenuation models with 0.1-second spectral acceleration predictions for soil classes A and B and for $M_w = 7.4$.

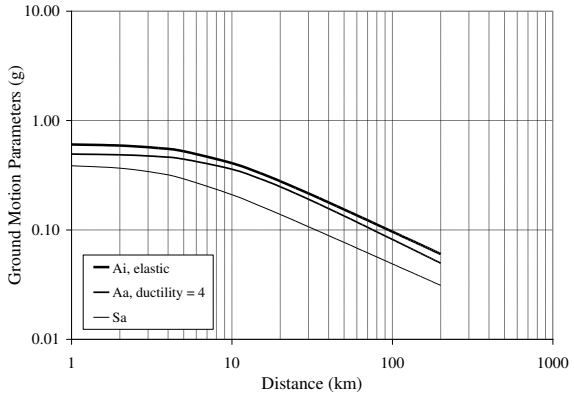

Figure 13: Comparison of 1.0-second elastic input energy-equivalent acceleration and inelastic (ductility = 4) absorbed energy-equivalent acceleration predictions from the proposed attenuation models with 1.0-second spectral acceleration predictions for soil classes A and B and for $M_w = 7.4$.

When comparing attenuation of the various parameters as a function of distance, the A_a/S_a ratio is expected to increase with distance according to Chou and Uang (2000). However, in the present study, this ratio is seen in Figs. 12 and 13 to be fairly uniform at all distances greater than around 10 km. Predicted A_i levels are higher than both A_a and S_a at all distances but the differences between A_a and A_i decrease at longer periods.

6.2 Comparison of the Proposed Model with Western U.S. Models

Absorbed Energy

Chou and Uang (2000) established ground-motion prediction equations for absorbed energy-equivalent velocity (V_a) for the Western U.S. using a two-stage regression analysis procedure. The geometric mean of the two horizontal

components of each ground motion recording was used in the study by Chou and Uang (2000) and the functional form of their attenuation model was similar to the one used here. A comparison of the proposed attenuation relationship predictions for a ductility factor of 4 with those of Chou and Uang (2000) is presented in Figs. 14 and 15 for an event with moment magnitude, M_w, of 7.4 and for soil classes A and B. The proposed attenuation model predicts generally similar levels of absorbed energy-equivalent acceleration (A_a) as the model by Chou and Uang (2000) at both periods, 0.1 and 1.0 seconds, as is seen in the figures. At short distances (say R < 10 km), the model by Chou and Uang (2000) predicts slightly higher 1.0-second A_a mean levels compared to the proposed model. In general, though, the Western U.S. model predictions are within one standard deviation of the mean predictions from the proposed model.

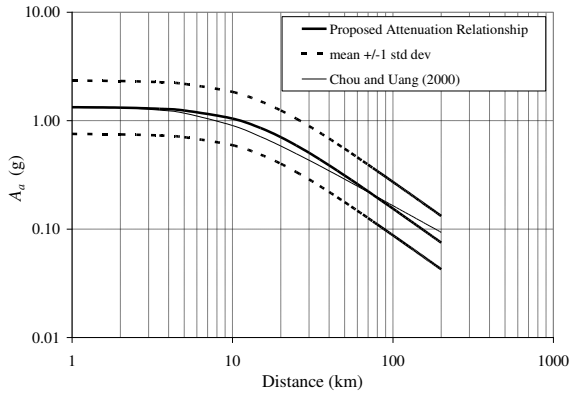

Figure 14: Comparison of predictions from the proposed attenuation model with those from a Western U.S. model for 0.1-second inelastic A_a (ductility = 4) for soil classes A and B and for M_w = 7.4.

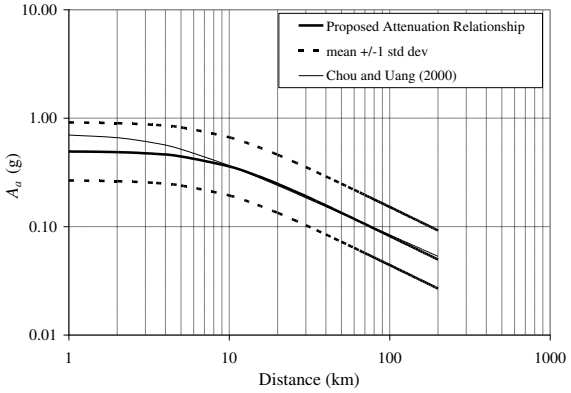

Figure 15: Comparison of predictions from the proposed attenuation model with those from a Western U.S. model for 1.0-second inelastic A_a (ductility = 4) for soil classes A and B and for $M_w = 7.4$.

In Fig. 16, predicted A_a spectra based on the proposed attenuation model are compared with the Western U.S. model of Chou and Uang (2000) at distances of 20, 60, and 150 km. Predictions of the mean absorbed energy-equivalent acceleration (A_a) spectra from the two attenuation models are very similar deviating only very slightly at longer distances than around 60 km. Again, though, the Western U.S. model predictions of mean A_a spectra lie well within one standard deviation of the predicted mean spectra based on the proposed model.

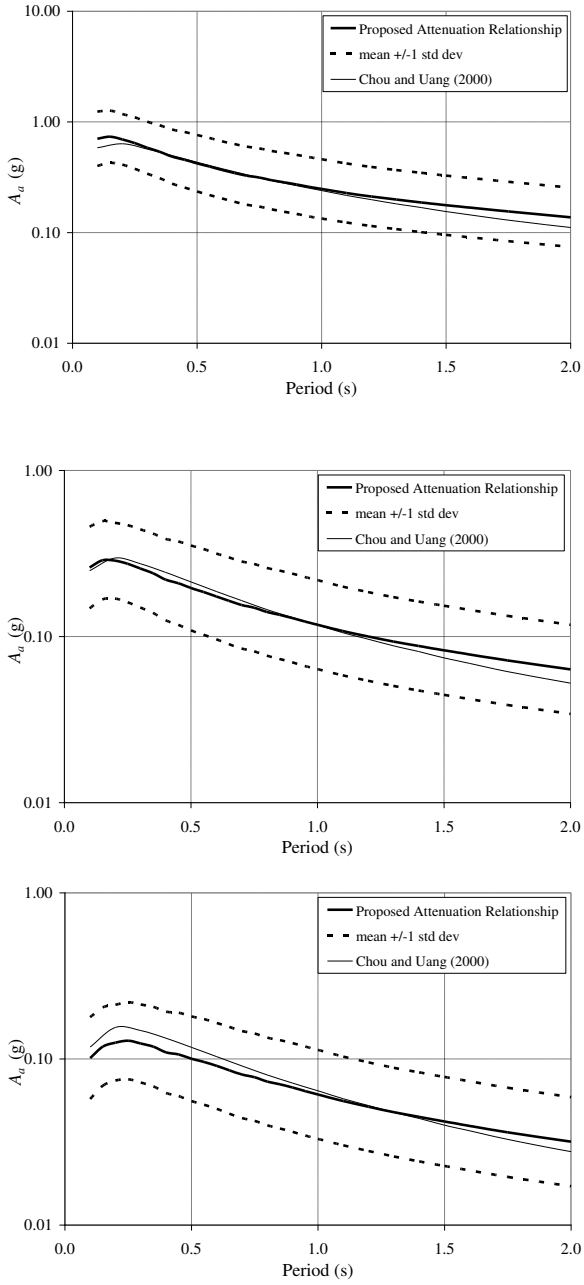

Figure 16: Comparison of predicted inelastic A_a spectra (ductility = 4) based on the proposed attenuation model with those based on a Western U.S. model for distances (20, 60, and 150 km) for soil classes A and B and for M_w = 7.4.

Input Energy

Lawson (1996) established ground-motion prediction equations for input energy-equivalent velocity (V_i) for the Western U.S. using a similar regression model to that used here. That study was based on 126 ground motion records. The V_i value used there was based on the larger of the two horizontal components rather than the geometric mean of the two components that is used here. Chapman (1999) also proposed ground-motion prediction equations for V_i for the Western U.S. based on 303 ground motion records. The geometric mean of two horizontal components was used in that study. A comparison of the proposed attenuation relationship predictions for elastic A_i with those of Lawson (1996) and Chapman (1999) is presented in Figs. 17 and 18 for an event with moment magnitude, M_w, of 7.4 and for soil classes A and B. For the 1.0-second predictions, both of the models based on Western U.S. data generally predict somewhat higher levels of input energy-equivalent acceleration, A_i, at all distances compared with the proposed attenuation model. At the shorter period (0.1 seconds), the Western U.S. models predict higher A_i levels only over very large distances.

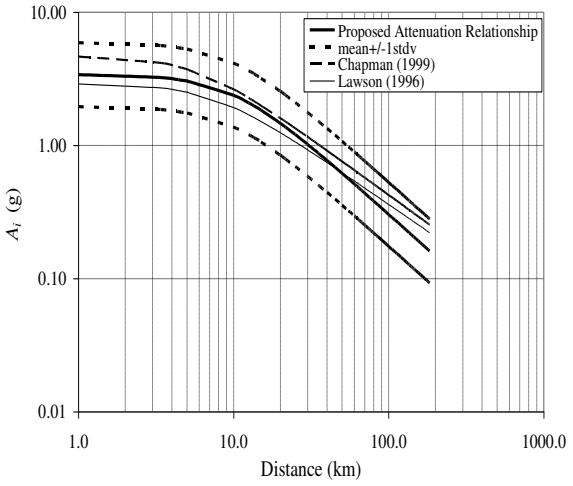

Figure 17: Comparison of predictions from the proposed attenuation model with those from two Western U.S. models for 0.1-second elastic A_i for soil classes A and B and for $M_w = 7.4$.

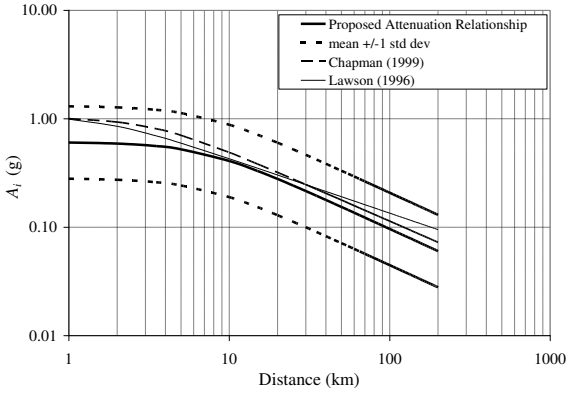

Figure 18: Comparison of predictions from the proposed attenuation model with those from two Western U.S. models for 1-second elastic A_i for soil classes A and B and for $M_w = 7.4$.

In Fig. 19, predicted A_i spectra based on the proposed attenuation model are compared with the two Western U.S. models of Lawson (1996) and Chapman (1999) at distances equal to 20, 60, and 150 km. Predictions of the mean input

energy-equivalent acceleration (A_i) spectra from the three attenuation models are generally quite similar with largest deviations at the 150 km distance. The Western U.S. model predictions of mean A_i spectra lie well within one standard deviation of the predicted mean spectra based on the proposed model, except at the 150 km distance where especially at short periods, the Western U.S. model predictions are almost one standard deviation above the mean spectra from the proposed model.

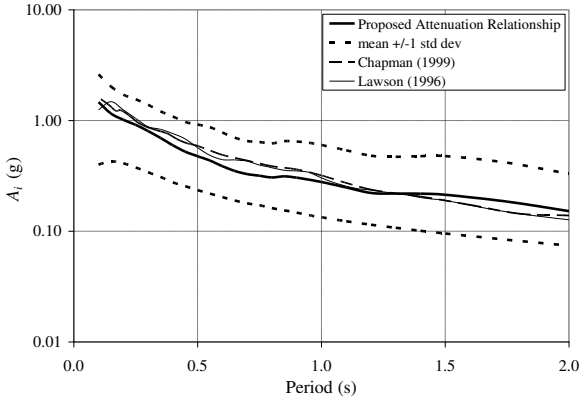

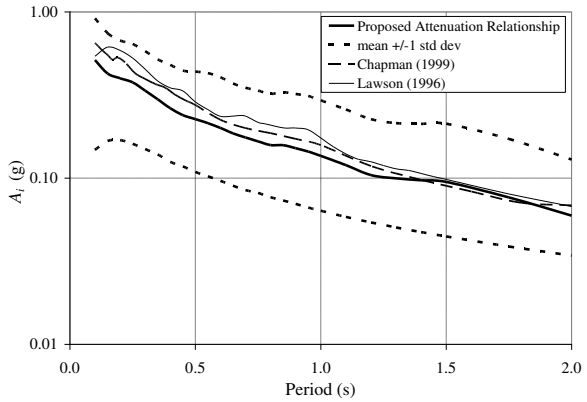

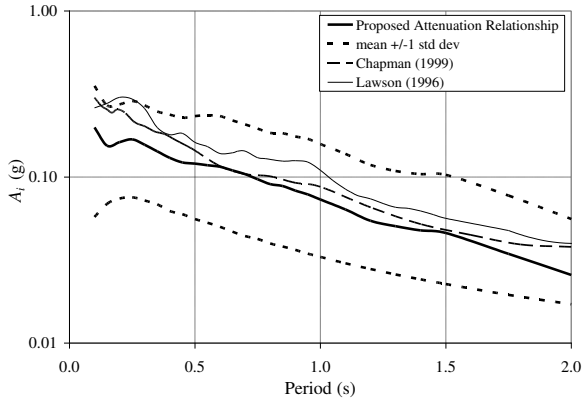

Figure 19: Comparison of predicted elastic A_i spectra based on the proposed attenuation model with those based on two Western U.S. models for distances (20, 60, and 150 km) for soil classes A and B and for M_w = 7.4.

6.3. Amplification of Energy-Based Parameters due to Site Conditions

There are almost no previous studies except that of Chou and Uang (2000) that address amplification of energy-based parameters due to site/soil conditions. Here, two factors, F_a' and F_v', for short-period and mid-period amplification of energy-based acceleration are defined in a manner quite similar to the amplification factors, F_a and F_v, employed in the NEHRP Provisions (NEHRP, 2001) for amplification of spectral acceleration for different site classes (relative to a reference site class). We consider amplification factors for A_a for site classes C and D relative to site classes A and B taken together as the reference site class. The amplification factor, F_a', is defined at a period of 0.2 seconds while F_v' is defined at a period of 1.0 second. Based on predicted levels of the selected

energy-based acceleration parameter for the different site classes, these two soil amplification factors are computed as follows:

$$F'_a = \frac{A_{a,soil}\ at\ T = 0.2\,\text{sec}}{A_{a,(A+B)}\ at\ T = 0.2\,\text{sec}},\ F'_v = \frac{A_{a,soil}\ at\ T = 1.0\ \text{sec}}{A_{a,(A+B)}\ at\ T = 1.0\ \text{sec}} \qquad (9)$$

where the numerator in the two factors refers to predicted level of A_a (for a ductility of 4) for the site class (C or D) under consideration. Similarly, amplification factors for the elastic input energy-equivalent acceleration (A_i) were defined in a similar manner to that given by Eq. (9).

Table 5 shows amplification factors for the two energy-based parameters for site classes C and D at periods of 0.2 and 1.0 seconds. Similar patterns related to the amplification are observed as with spectral acceleration in NEHRP (2001). Greater amplification levels for A_a and A_i are generally noted at the longer periods and for the softer soil classes.

The establishment of amplification factors in this manner makes it relatively easy to account for site effects in studies involving energy-based parameters (such as in energy-based probabilistic seismic hazard analysis). However, additional studies are required on amplification of energy demands that consider various levels of input motion and examine other natural periods a well.

Table 5: Amplification factors, F_a' and F_v', for energy-based parameters for site classes C and D at periods of 0.2 and 1.0 seconds, respectively.

	A_a Amplification Factors		A_i Amplification Factors	
Site Class	F_a'	F_v'	F_a'	F_v'
C	1.2	1.3	1.3	1.2
D	2.0	2.7	2.1	2.8

7. CONCLUSIONS

The severity of earthquake ground shaking can be characterized using energy-based intensity measures such as absorbed energy and input energy. Such energy-based parameters can serve as alternatives to more conventional strength-based parameters such as spectral acceleration. New ground-motion prediction equations have been developed for 5%-damped absorbed energy-equivalent acceleration (A_a) and input energy-equivalent acceleration (A_i) for periods up to 4 seconds. A mixed effects model has been employed here to establish these relationships that accounts for inter- and intra-event variability. Coefficients for use with the proposed attenuation models are presented for inelastic A_a predictions for a ductility factor of 4 and for elastic A_i predictions.

This study is region-specific as only recordings from earthquakes that have occurred in Northwestern Turkey have been employed in developing the ground-motion prediction equations. Comparing predictions of energy-based acceleration parameters for Northwestern Turkey with a strength-based parameter

(spectral acceleration, S_a), it was found that the energy demand parameters were generally greater with elastic A_i demands highest. Also, inelastic A_a demands were higher than S_a in part because inelastic absorbed energy includes contributions from hysteretic energy. In contrast with the findings of Chou and Uang (2000), the A_a/S_a ratio was not found to increase with distance in the present study; this ratio was almost the same at all distances.

When the proposed model was compared to predictions based on Western U.S. empirical attenuation models for shallow crustal zones not very different from that for Northwestern Turkey, it was found that the Western U.S. models generally predicted similar energy demands to those with the proposed model. However, the comparisons of the elastic response spectra in Özbey et al (2004) show large differences between Northwestern Turkey and Western US predictions. There is an apparent inconsistency as Western US predictions are inconsistent (Sari (2003), See Figure 4.4).

The proposed attenuation model predicts generally similar levels of inelastic absorbed energy-equivalent acceleration (A_a) to the Western U.S. models at both periods, 0.1 and 1.0 seconds. The Western U.S. models generally predicted slightly higher levels of input energy-equivalent acceleration (A_i) compared to the proposed attenuation model.

For the two energy-based parameters studied, amplification factors, F_a' and F_v', were defined and proposed for site classes C and D to account for amplification of motions due to site conditions. These factors, F_a' and F_v', correspond to soil amplification factors at 0.2 and 1.0 second periods, respectively. As expected, greater amplification levels for A_a and A_i were generally noted at the longer periods and for the softer soil class (site class D). Both the energy-based acceleration parameters, A_a and A_i, were found to experience similar levels of soil amplification at the two periods studied.

REFERENCES

Abrahamson, N. A. and Youngs, R. R. (1992). "A Stable Algorithm for Regression Analyses using the Random Effects Model," Bull. Seism. Soc. Am., 82, 505-510.

Abrahamson, N A and Silva, W. J. (1997). "Empirical response spectral attenuation relations for shallow crustal earthquakes". Seismological Research Letters; 68(1): 94-127.

Ambraseys, N. N. (1970). "Some Characteristic Features of the Anatolian Fault Zone," Tectonophysics, Vol. 9, pp. 143-165.

Boore, D. M. and Joyner, W.B. (1982). "The empirical prediction of ground motion," Bull. Seism. Soc. Am., 72, S269–S268.

Çelebi, M., Toprak, S. and Holzer, T. (1999). "Strong-Motion, Site-Effects and Hazard Issues in Rebuilding Turkey: In Light of the 17 August, 1999 Earthquake and its Aftershocks," Proceedings ITU-IAHS International Conference on the Kocaeli Earthquake, 17 August 1999, pp. 93-110, Istanbul, Turkey.

Chapman, M. C. (1999). “On the Use of the Elastic Input Energy for Seismic Hazard Analysis,” Earthquake Spectra, Vol. 15, pp. 607-637.

Chou C. C. and Uang C. M. (2000). “An Evaluation of Seismic Energy Demand: An attenuation approach,” Pacific Earthquake Engineering Research Center Report 2000/04, College of Engineering University of California, Berkeley.

Decanini, Luis D., and Fabrizio Mollaioli. 2001. “An Energy-Based Methodology for the Assessment of Seismic Demand.” Soil Dynamics and Earthquake Engineering 21(2): 113–37.

Dewey, W. J. (1976). “Seismicity of Northern Anatolia,” Bulletin of the Seismological Society of America, Vol. 66.

Dindar, Ahmet Anıl et al. 2013. “Development of Earthquake Energy Demand Spectra.” Earthquake Spectra 33(3): 1075–1100.

Lawson, R. S. (1996). “Site-dependent Inelastic Seismic Demands,” Ph.D. Dissertation, Stanford University, Stanford, California.

López-Almansa, F., A. U. Yazgan, and A. Benavent-Climent. 2013. “Design Energy Input Spectra for High Seismicity Regions Based on Turkish Registers.” Bulletin of Earthquake Engineering 11(4): 885–912.

Ma, Cuiling. 2019. “Energy-Based Seismic Design Method for EBFs Based on Hysteretic Energy Spectra and Accumulated Ductility Ratio Spectra.” Advances in Civil Engineering.

Ma, Cuiling, Qiang Gu, and Guohua Sun. 2019. “Mathematical Expression of Design Hysteretic Energy Spectra Based on Chinese Soil Type.” Mathematical Problems in Engineering.

Merter, Onur, Özgür Bozda, and Mustafa Düzgün. 2012. “Energy-Based Design of Steel Structures According to the Predefined Interstory Drift Ratio.” Teknik Dergi/Technical Journal of Turkish Chamber of Civil Engineers 23(DECEMBER): 1573–93.

Ozsarac, Volkan, Shaghayegh Karimzadeh, Murat Altug Erberik, and Aysegul Askan. 2017. "Energy-Based Response of Simple Structural Systems by Using Simulated Ground Motions." Procedia Engineering 199: 236–41. http://dx.doi.org/10.1016/j.proeng.2017.09.009.

NEHRP (2001). "NEHRP Recommended Provisions for Seismic Regulations for New Buildings and other Structures," Part 1 – Provisions, Federal Emergency Management Agency, FEMA 368.

Orgulu, G. and Aktar, M. (2001). "Regional Moment Tensor Inversion for Strong Aftershocks of the August 17, 1999 Izmit Earthquake (Mw=7.4)," Geophysical Research Letters, 28, No. 2, 371-374.

Özbey, C., Sari, A., Manuel, L., Erdik, M. and Fahjan, Y. (2004). "An empirical attenuation relationship for Northwestern Turkey ground motion using a random effects approach," Soil Dynamics and Earthquake Engineering, Vol. 24, No. 2, pp. 115-125, February 2004.

Rathje, E.M., Stokoe, K.H., and Rosenblad, B.L. (2003). "Strong Motion Station Characterization and Site Effects During the 1999 Earthquakes in Turkey,"

Earthquake Spectra, Earthquake Engineering Research Institute, 19(3), pp. 653-676.

Sari, A. (2003). “Energy Considerations in Ground Motion Attenuation and Probabilistic Seismic Hazard Studies Site,” Ph.D. Dissertation, University of Texas, Austin, TX.

Sari, A. and Manuel. L.(2002). “Strength and Energy Demands from the August 1999 Kocaeli Earthquake Ground Motions,” Paper 661, Proceedings of the 7th U.S. National Conference on Earthquake Engineering, Boston.

Seneviratna, G. D. P. K. and Krawinkler, H. (1997). “Evaluation of Inelastic MDOF Effects for Seismic Design,” Department of Civil Engineering, Stanford University, CA.

Shiwua, Aondowase John, and Yuri Rutman. 2016. “Assessment of Seismic Input Energy By Means of New Definition and the Application To Earthquake Resistant Design.” Architecture and Engineering 1(4).

Ye, Lieping, Guangyu Cheng, Zhe Qu, and Xinzheng Lu. 2009. “Study on Energy-Based Seismic Design Method and Application on Steel Braced Frame Structures.” Journal of Building Structures 33(11): 36–45.

Uang, C. M. and Bertero V. V. (1988). “Use of Energy as a Design Criterion in Earthquake-Resistant Design,” Report No: UCB/EERC-88/18, Earthquake Engineering Research Center, Collage of Engineering, University of California at Berkeley.